High-Quality Fe and γ-Fe_2O_3 Magnetic Thin Films from an Epoxide-Catalyzed Sol−Gel Process

Chi-Dong Park, Donny Magana, and A. E. Stiegman*

Department of Chemistry and Biochemistry and the Materials Research and Technology Center (MARTECH), Florida State University, Tallahassee, Florida 32306

Received July 21, 2006. Revised Manuscript Received November 14, 2006

High-quality amorphous Fe^{3+} oxide/hydroxide thin films were fabricated through an epoxide-catalyzed sol−gel process in which hexaaquo Fe^{3+} salts were condensed in an alcoholic medium with propylene oxide. After addition of the propylene oxide, but prior to gelation, the solution was spin-coated onto quartz disks. The Fe^{3+} oxide/hydroxide films that formed were extremely uniform and homogeneous with a film thickness of ~0.1 μm. Processing of these films under either oxidizing or reducing conditions allows them to be converted into magnetic iron or iron oxide phases. Calcination under an inert atmosphere at 600 °C cleanly converts the Fe^{3+} oxide/hydroxide gel to hematite (α-Fe_2O_3), while reduction of either the Fe^{3+} gel films directly or the hematite films in a dilute H_2 flow produces metallic iron. The iron films produced from either of these methods are characterized by a distribution of submicrometer particles on the surface. The metallic iron particles can ultimately be converted to well-formed maghemite (γ-Fe_2O_3) particles through slow reoxidation. Magnetic susceptibility measurements taken parallel and perpendicular to the surface indicate that both the iron and the maghemite are anisotropic, showing evidence of long-range interactions parallel to the surface.

Introduction

Iron oxide thin films are of technological interest for their potential magnetic, optical, and catalytic applications. Thin films of various iron oxide phases (i.e., α-and γ-Fe_2O_3 and Fe_3O_4) have most commonly been made using vacuum deposition techniques such as sputtering, chemical vapor, and arc-plasma spray deposition.[1−7] Solution chemical (sol−gel) approaches have also been exploited successfully, albeit less frequently, to produce high-quality films. These approaches have generally involved the hydrolysis of organometallic precursors such as alkoxides or acetylacetonates using methods originally developed by Schroeder and Dislich or the use of soluble iron salts with organic gelling agents such as glycols or polymeric phases.[8−19]

Recently, Gash et al. have reported a new technique for the sol−gel synthesis of a wide range of metal oxides.[20−22] In their approach, gel formation occurs through the epoxide-catalyzed condensation of metals ions with an aquated inner coordination sphere. As shown by these authors, the reaction is quite general, producing high-quality gels from a wide range of transition and main group metal ions and affords considerable synthetic flexibility as to composition and the final crystalline phase.[23]

To date, there have been no reports of the gels' applicability for thin film formation. In this study, we report that in the case of gels made from aquated Fe^{3+} ions by this process, high-quality thin films on a fused quartz substrate can be readily produced. These films can, in turn, be thermally processed in a reductive or oxidative environment to produce metallic or oxidized films, which, in many cases, retain the film quality of the initial gel coating.

Experimental Procedures

Thin Film Fabrication. The films were formed from 0.64 M stock solutions of Fe^{3+} dissolved in ethanol (2.59 g of $Fe(NO_3)_3$•-

* Corresponding author. E-mail:stiegman@chem.fsu.edu.

(1) Akl, A. A. *Appl. Surf. Sci.* **2004**, *233*, 307.
(2) Akl, A. A. *Appl. Surf. Sci.* **2004**, *221*, 319.
(3) Aronniemi, M.; Lahtinen, J.; Hautojaervi, P. *Surf. Inter. Anal.* **2004**, *36*, 1004.
(4) Miller, E. L.; Paluselli, D.; Marsen, B.; Rocheleau, R. E. *Thin Solid Films* **2004**, *466*, 307.
(5) Pal, B.; Sharon, M. *Thin Solid Films* **2000**, *379*, 83.
(6) Peng, Y.; Park, C.; Laughlin, D. E. *J. Appl. Phys.* **2003**, *93*, 7957.
(7) Yubero, F.; Ocana, M.; Justo, A.; Contreras, L.; Gonzalez-Elipe, A. R. *J. Vac. Sci. Technol., A* **2000**, *18*, 2244.
(8) Armelao, L.; Granozzi, G.; Tondello, E.; Colombo, P.; Principi, G.; Lottici, P. P.; Antonioli, G. *J. Non-Cryst. Solids* **1995**, *193*, 435.
(9) Dislich, H. *Angew. Chem., Int. Ed. Engl.* **1971**, *10*, 363.
(10) Dislich, H.; Hinz, P. *J. Non-Cryst. Solids* **1982**, *48*, 11.
(11) Dislich, H.; Hussmann, E. *Thin Solid Films* **1981**, *77*, 129.
(12) Hida, Y.; Kozuka, H. *Thin Solid Films* **2005**, *476*, 264.
(13) Takahashi, N.; Kakuta, N.; Ueno, A.; Yamaguchi, K.; Fujii, T.; Mizushima, T.; Udagawa, Y. *J. Mater. Sci.* **1991**, *26*, 497.
(14) Tanaka, K.; Yoko, T.; Atarashi, M.; Kamiya, K. *J. Mater. Sci. Lett.* **1989**, *8*, 83.
(15) Chang, H. S. W.; Chiou, C. C.; Chen, Y. W.; Sheen, S. R. *J. Solid State Chem.* **1997**, *128*, 87.
(16) Kojima, K.; Miyazaki, M.; Mizukami, F.; Maeda, K. *J. Sol-Gel Sci. Technol.* **1997**, *8*, 77.
(17) Kordas, G.; Weeks, R. A.; Arfsten, N. *J. Appl. Phys.* **1985**, *57*, 3812.
(18) Sedlar, M. *Ceram. Int.* **1994**, *20*, 73.
(19) Tang, N. J.; Zhong, W.; Jiang, H. Y.; Wu, X. L.; Liu, W.; Du, Y. W. *J. Magn. Magn. Mater.* **2004**, *282*, 92.
(20) Gash, A. E.; Tillotson, T. M.; Satcher, J. H.; Hrubesh, L. W.; Simpson, R. L. *J. Non-Cryst. Solids* **2001**, *285*, 22.
(21) Gash, A. E.; Tillotson, T. M.; Satcher, J. H.; Poco, J. F.; Hrubesh, L. W.; Simpson, R. L. *Chem. Mater.* **2001**, *13*, 999.
(22) Tillotson, T. M.; Gash, A. E.; Simpson, R. L.; Hrubesh, L. W.; Satcher, J. H.; Poco, J. F. *J. Non-Cryst. Solids* **2001**, *285*, 338.
(23) Gash, A. E.; Satcher, J. H.; Simpson, R. L. *Chem. Mater.* **2003**, *15*, 3268.

10.1021/cm0617079 CCC: $37.00
Published on Web 01/24/2007

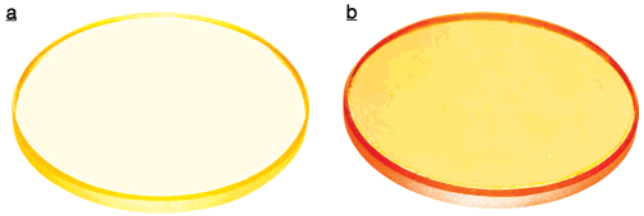

Figure 1. Thin films spin-coated on a 2.54 cm quartz disk of epoxide-catalyzed Fe^{+3} sol−gels (a) as-formed and (b) calcined at 600 °C.

$9H_2O$ (Aldrich) in 10 mL of absolute ethanol). After dissolution, 1 mL of proplyene oxide (Aldrich) was slowly added to 5 mL aliquots of the Fe^{3+} solution. The solution was allowed to react over a period of 2 min during which time it turned from red to dark brown. At this point, using a disposable pipette, 5 drops of the Fe^{3+} solution were dispensed on a quartz disk (2.5 cm) that had been placed on a spin-coater at ∼3000 rpm. The coated substrates were allowed to age for several days at room temperature prior to analysis. Film thickness was estimated from profilometry traces acquired over a section scored to remove the film down to the substrate.

Thermal Processing. Coated disks were placed in a tube furnace equipped with O_2 impermeable hoses under an N_2 flow and baked at 600 °C for a period of 6 h. Reduction to metallic iron was carried out in an analogous fashion under a flow of H_2 in N_2 ($H_2/N_2 = 0.2$ v/v) for 1 h. The Fe films were recovered by allowing them to cool to room temperature while still maintaining a reductive environment with the H_2/N_2 flow. Reoxidation to generate maghemite was performed by taking the just-reduced Fe films from 600 °C to room temperature at a rate of 5 °C/min under a flow of UHP grade N_2; the oxidant is believed to be trace O_2 (1 ppm in UHP N_2) in the N_2 stream, although some contribution from adventitious oxygen in the system cannot be ruled out.

Characterization. X-ray diffraction was performed on a Siemems D-500 X-ray diffractometer with nickel filtered Cu Kα ($\lambda = 1.540562$). The XRD patterns of thin films were recorded in the range of 20−70° (scan speed = 2°/min). The X-ray tube operated at 40 kV/30 mA. Microscopy was carried out by atomic force microscopy (AFM) and scanning electron microscopy (SEM). The AFMs were acquired in tapping mode at 290−360 kHz on a Digital Instruments Dimension 3000 equipped with silicon tips. The AFM images of thin films were processed using Nanoscope version 5.12 software. SEMs were carried out on a JEOL JSM 840 operated at 10 and 20 kV. The samples were coated with Au/Pd by sputtering. UV−vis spectroscopy was carried out on a Perkin-Elmer Lambda 900 spectrophotometer over a wavelength range of 200−900 nm. Spectra were acquired in transmission mode through the quartz deposited thin film. The magnetic properties of the films were measured on a Quantum Design XL-7 superconducting quantum interference device (SQUID).

Results and Discussion

Aged thin films formed from spin-coating propylene oxide-catalyzed Fe^{3+} sol−gel solutions on a quartz substrate appear, qualitatively, continuous and extremely homogeneous (Figure 1a). The apparent smoothness is also observable on a microscopic scale in images obtained from atomic force microscopy (AFM) and scanning electron microscopy (SEM). The surface, as imaged by tapping mode AFM (Figure 2), is very flat with a measured root-mean-squared (rms) roughness of 2.30 nm and is typified by an array of small peaks ∼1 nm in width. The SEM (not shown) showed the film to be essentially featureless and uniform with no obvious

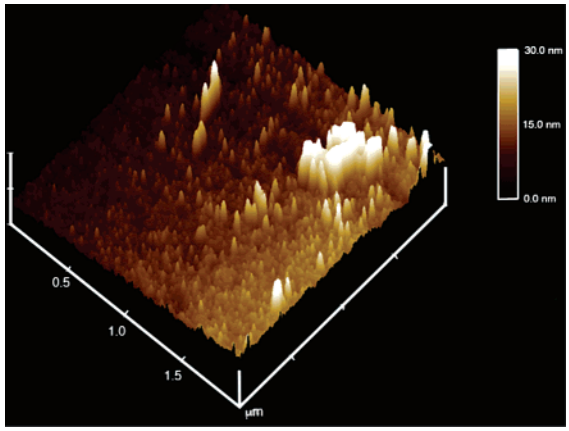

Figure 2. AFM image of as-formed Fe^{+3} oxide/hydroxide thin film (high areas on right are interpreted as surface debris).

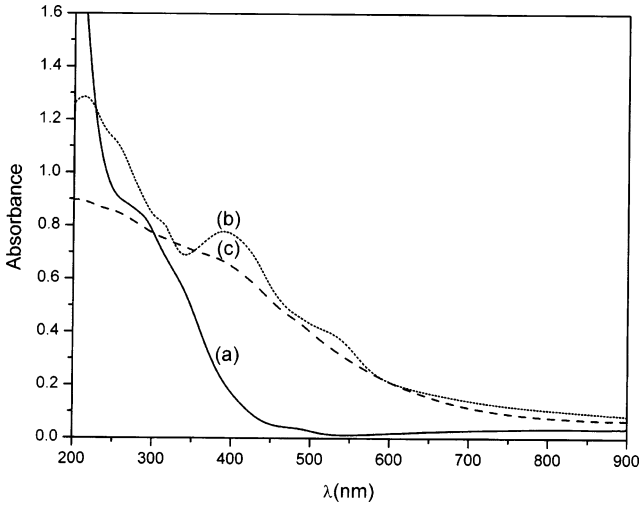

Figure 3. UV−vis spectrum of Fe^{3+} oxiode/hydroxide thin films (a) as-synthesized, (b) after calcination at 600 °C under N_2 to form α-Fe_2O_3, and (c) calcination under N_2 followed by reduction under dilute H_2 to form Fe.

cracks or voids that are often seen in sol−gel derived thin films due to shrinkage during drying. The thickness of the as-prepared film, determined from profilometry, was found to be 119 nm. Taken together, these results suggest that the film forming characteristics of the epoxide-catalyzed Fe^{3+} sol−gel are excellent, producing very high-quality thin films on both a macro- and microscopic scale. As reported by Gash et al., the product of the propylene oxide-catalyzed gelation of $Fe(H_2O)_6^{+3}$ is a largely amorphous iron oxide/hydroxide phase known as ferrihydrite that also contains organic products of the epoxide catalysis.[23] Consistent with retention in the thin film of this essentially amorphous phase, no X-ray diffraction was observed. The electronic spectrum, collected in transmission mode through the film (Figure 3a) is typical of related iron oxide hydroxide species (e.g., goethite and lepidocrocite) with relatively strong bands at $\lambda < 500$ nm associated with Fe(III) ligand field transitions.[24]

While thin films of Fe^{3+} oxide/hydroxide gels are not currently of direct technological interest, we have determined that under carefully controlled conditions, it is possible to convert these films into potentially useful metallic or oxidic phases while retaining much of the quality of the original

(24) Sherman, D. M. *Phys. Chem. Miner.* **1985**, *12*, 161.

Scheme 1

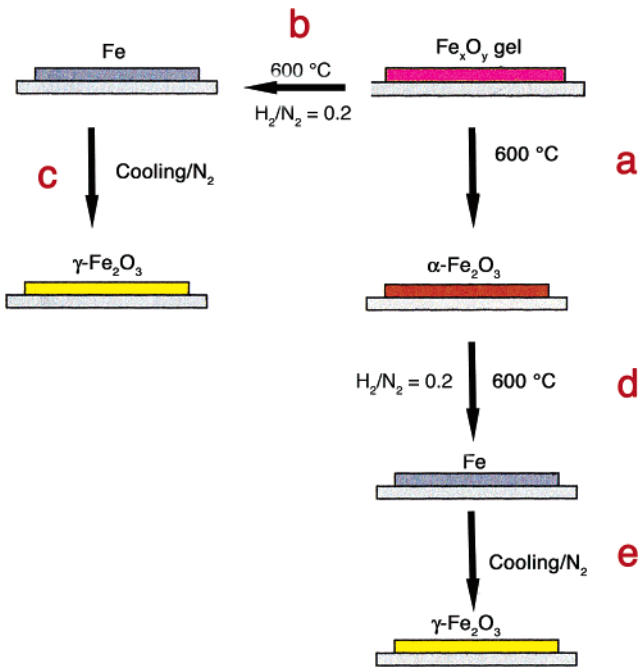

Fe^{3+} gel film. As shown in Scheme 1, the amorphous Fe^{3+} oxide/hydroxide thin film can either be oxidized to α-Fe_2O_3 (Scheme 1, pathway a) or reduced to metallic Fe (Scheme 1, pathway b). Once formed, these films can be further converted through sequential oxidation and reduction processes to magnetic γ-Fe_2O_3.

Oxidation to α-Fe_2O_3 (Scheme 1, Pathway a). Calcination of the Fe_xO_y gel films at 600 °C under either air or an inert atmosphere results in a color change from pale to dark orange (Figure 1b). The thickness of the film after calcination is ∼49 nm, suggesting that the gel derived films shrink substantially upon thermal processing. The X-ray diffraction pattern of the calcined gel indicates that it has been converted to α-Fe_2O_3 (Figure 4a). This conversion is further confirmed by the UV−vis spectrum (Figure 3b), which is identical to that reported for bulk hematite with an intense, well-resolved band at 430 nm associated with the ligand field $^6A_1 \rightarrow {}^4E$, $^4A_1$ transitions and a resolved shoulder at 530 nm that has been assigned to the $2(^6A_1) \rightarrow 2(^4T_1(4G))$ pair excitation transition.[25] Interestingly, the calcination product of the iron gel thin films under an inert atmosphere yields different products from those observed with bulk material where magnetite and hematite are produced under inert and oxidizing atmospheres, respectively. The origin of this difference in behavior is not known for certain; however, the as-synthesized iron oxide gel contains a significant amount of organic material (17% C for samples dried under N_2 at 75 °C for 24 h) that can act as reductants to convert the Fe^{3+} to Fe^{2+} to yield magnetite during calcination. In the thin film, these organic reductants may be lost rapidly during heating due to the high surface area and small volume, which causes Fe to remain in the +3 oxidation state.

The surface morphology of the calcined films, as analyzed by AFM (Figure 5), was found to be significantly rougher

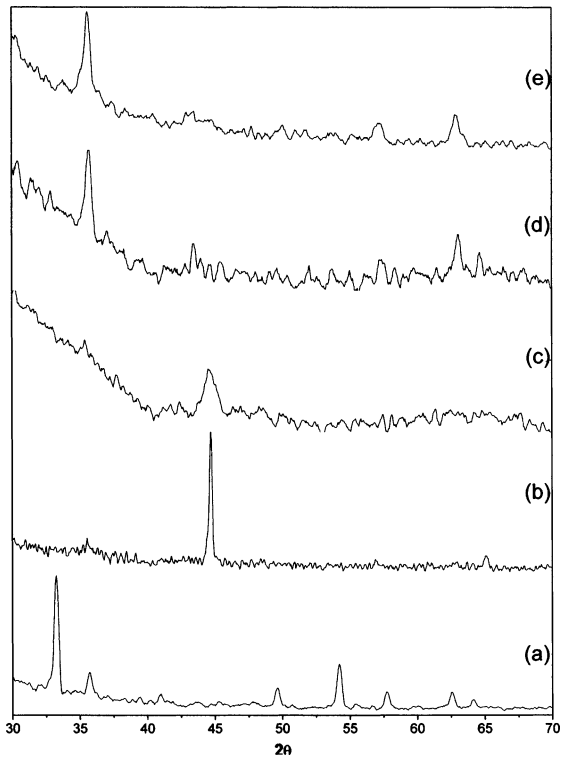

Figure 4. Powder X-ray diffraction from Fe^{3+} oxide/hydroxide gel thin films after (a) calcination at 600 °C under N_2 (Scheme 1, pathway a), (b) reduction under dilute H_2 (Scheme 1, pathway b), (c) calcination under N_2 followed by reduction under dilute H_2 (Scheme 1, pathway d), (d) reoxidation of Fe (Scheme 1, pathway c), and (e) reoxidation of Fe (Scheme 1, pathway e).

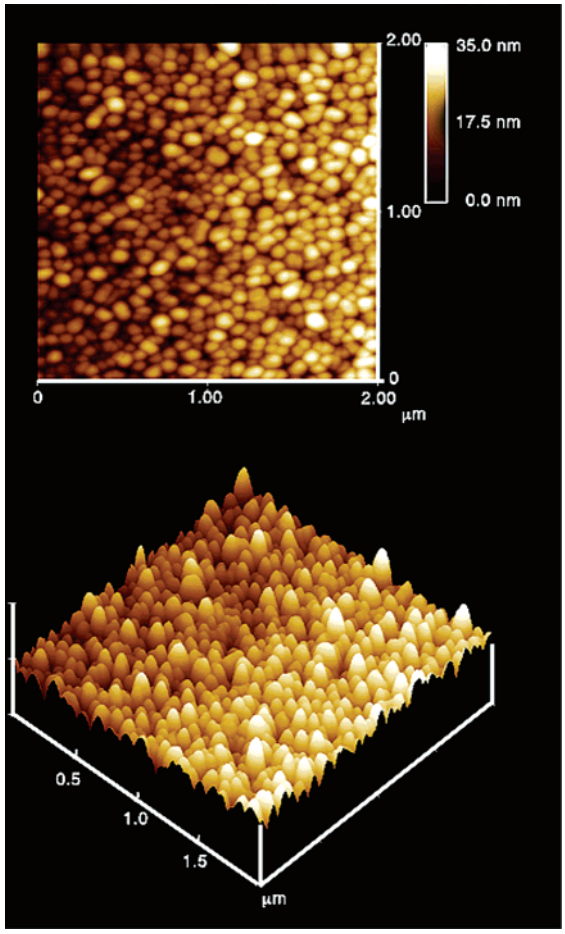

Figure 5. AFM image of α-Fe_2O_3 thin film formed from the calcination of thin films made from Fe^{3+} oxide/hydroxide gels.

(25) Sherman, D. M.; Waite, T. D. *Am. Miner.* **1985**, *70*, 1262.

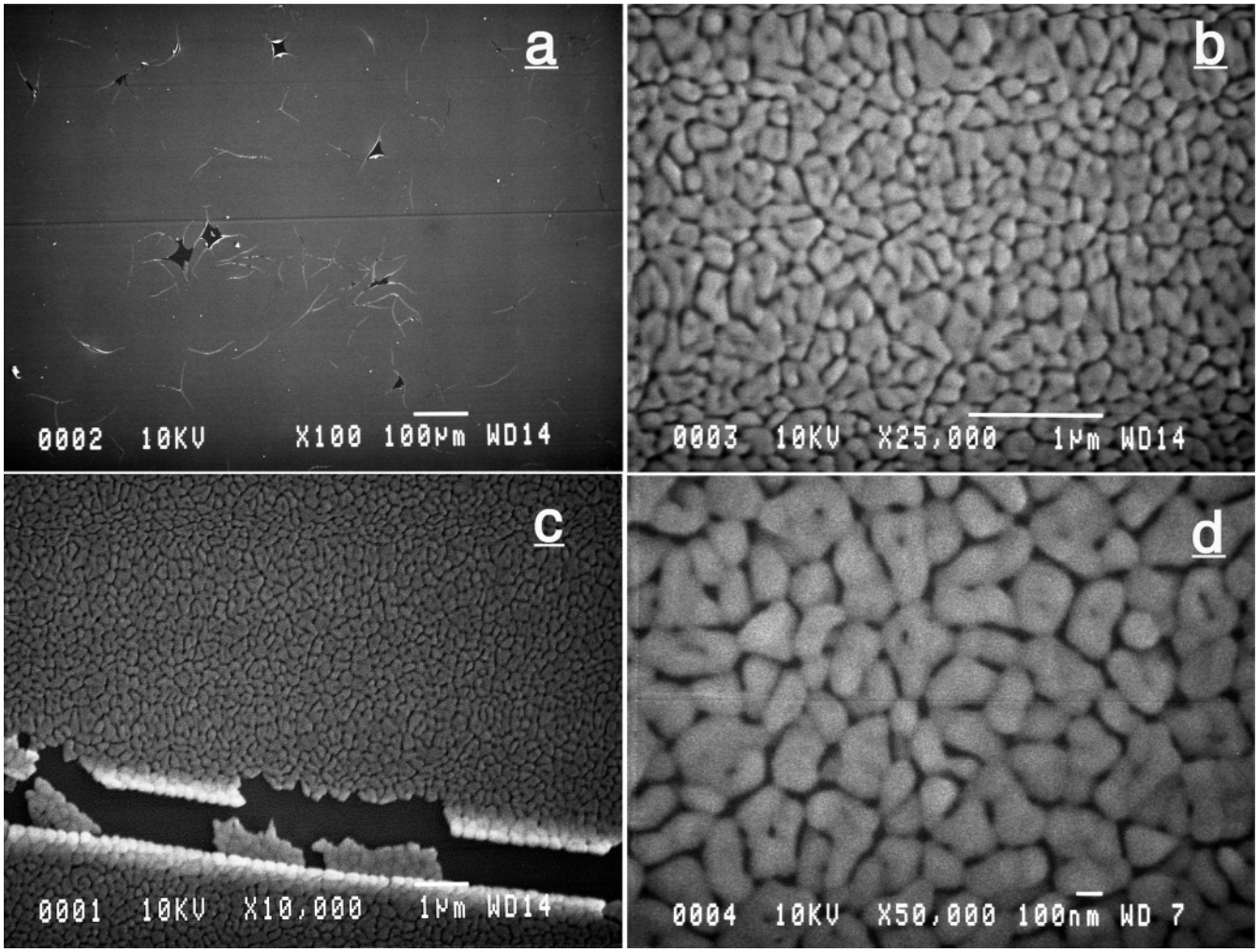

Figure 6. SEM images of α-Fe_2O_3 thin films from calcination of Fe^{+3} oxide/hydroxide thin films at (a) ×100, (b) ×25 000, (c) ×10 000 showing scored section, and (d) ×50 000 magnification.

than the gel with an rms roughness of 4.63 nm. The surface exhibits a granular structure with a mean grain diameter of ∼100 nm. Scanning electron microscopy of the surface at (×100; Figure 6a) shows the surface to be uniformly covered by the film with some cracks and pinholes observable in the image. At progressively high magnifications, a brain-coral morphology becomes apparent with regions ∼200 nm in diameter separated by what appears to be troughs of ∼20 nm. A score mark across the film is imaged in Figure 6c, which shows that fragmentation occurs along the spaces between the globular regions, supporting the assertion that they are void spaces (troughs) in the film. Estimates of crystallite size obtained from applications of the Scherer equation to the XRD yields an average size of ∼28 nm, which suggests that the observed microstructure is composed of smaller Fe_2O_3 crystallites. Interestingly, the microscopic morphology we observe compares closely with those reported for films made from organic gelling agents, in particular, that observed by Hida and Kozuka for hematite films made from solutions of ferric nitrate with polyvinylpyrrolidone (PVP) and for magnetite films fabricated by Chang et al. from Fe^{2+} and Fe^{3+} salts using ethylene glycol and citric acid as gelling agents.[12,15] This similarity may arise from the relatively large amount of residual organic material, which remains in the iron gels coatings. If, as the gel dries, the organic phases separate into distinct regions, their removal with calcinations may leave the observed void space.

Reduction to Metallic Fe. Direct reduction of the thin films Fe^{3+} oxide/hydroxide gel (Scheme 1, pathway b) in a dilute, reducing atmosphere (H_2/N_2 = 0.2 v/v) at 600 °C results in the formation of a single crystalline phase as indicated by the XRD (Figure 4b), which proved to be metallic iron as indicated by the characteristic diffraction pattern with an intense [110] reflection and weaker [200] reflection observed at 2θ = 44.7 and 65°, respectively. Obviously, any amorphous phases present will not be detectable by XRD analysis. SEM imaging of the film surface at low magnification indicates that it is quite uniform; however, at higher magnifications (Figure 7), it becomes evident that the film is composed of irregularly shaped iron particles distributed rather uniformly across the surface. The particles as formed cover a range of sizes with the small particles appearing to be on the order of ∼100 nm and the larger particles being in the 400−500 nm range. The fact that the particles are so widely dispersed on the surface with interparticle distances on the order of several hundreds of nanometers in most cases is likely due to mass loss and shrinkage as the gel is heated and reduced.

Metallic iron films were also produced from reduction of the hematite films generated from oxidation of the Fe^{3t} oxide/

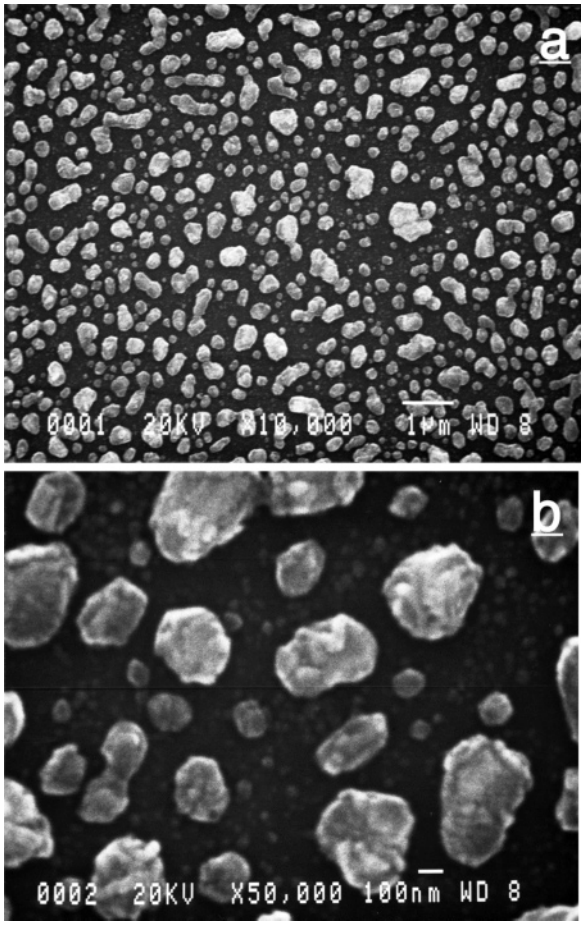

Figure 7. SEM images at (a) ×10 000 and (b) ×50 000 Fe particles made from the reduction of Fe^{3+} oxide/hydroxide thin films.

hydroxide gels (Scheme 1, pathway d). The reduction was carried out under the same conditions used to reduce the Fe^{3+} oxide/hydroxide gel: 600 °C under a dilute hydrogen flow (H_2/N_2 = 0.2 v/v) for a period of 60 min. These conditions resulted in complete reduction to metallic Fe as indicated by the XRD (Figure 4c). Both the AFM and the SEM analyses (Figure 8) show the surface to be composed of submicrometer Fe particles dispersed relatively uniformly across the surface. Qualitatively, the surface is similar in appearance to films produced from direct reduction of the Fe^{3+} oxide/hydroxide gel, but the iron particles are much more uniform in size and more evenly dispersed. Average grain size analysis of the AFM image gives a mean diameter of 223 nm. The broadness of the [110] reflection in the XRD, however, indicates that the materials are poorly crystalline, in comparison to metallic Fe produced through direct reduction of the Fe^{3+} oxide/hydroxide gel (Scheme 1, pathway b), even though the observed particles are of a similar size. Scrutiny of the AFM and SEM image (Figure 8) shows no faceting, and the AFM indicates that the individual particles have a substructure, which is consistent with the irregular particles being composed of an agglomeration of small crystallites.

Oxidation to γ-Fe_2O_3. Use of controlled processing conditions on the metallic iron films produced either from direct reduction of the Fe^{3+} gel or from reduction of the hematite made from the gel could be converted to maghemite, the ferrimagnetic γ phase of Fe_2O_3. This phase is of technological interest due to its extensive application in magnetic storage media. Commercially, maghemite is made from hematite, which is first reduced to magnetite and then reoxidized to maghemite.[26] For the Fe^{3+} oxide/hydroxide gel derived thin films, however, we were never successful in achieving a controlled reduction to magnetite. This contrasts with other sol−gel techniques in which magnetite could be produced directly.[14,15,18]

Reoxidation of the metallic Fe films containing distinct Fe particles (Scheme 1, pathways b and d) was carried out by turning off the hydrogen flow after reduction and allowing the films to cool from 600 °C to room temperature at a rate of 5 °C/min under a stream of dry N_2 (UHP, 1 ppm O_2). The very low oxygen content and the long oxidation period produced maghemite from both of the particulate Fe films.

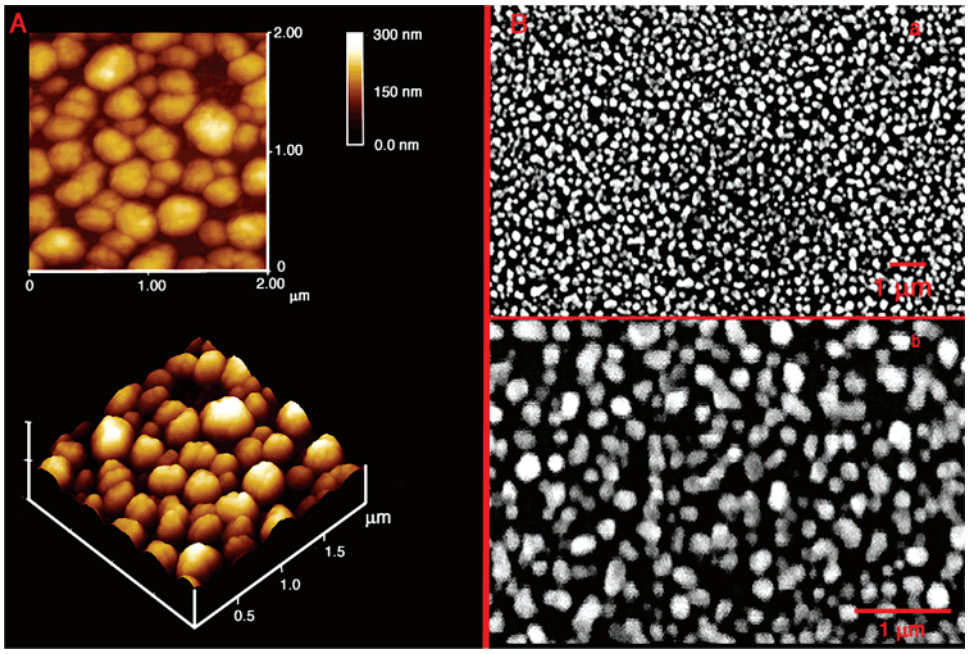

Figure 8. (A) AFM image and (B) SEM image at (a) ×10 000 and (b) ×25 000 magnification of the surface of metallic Fe formed from Scheme 1, pathway d.

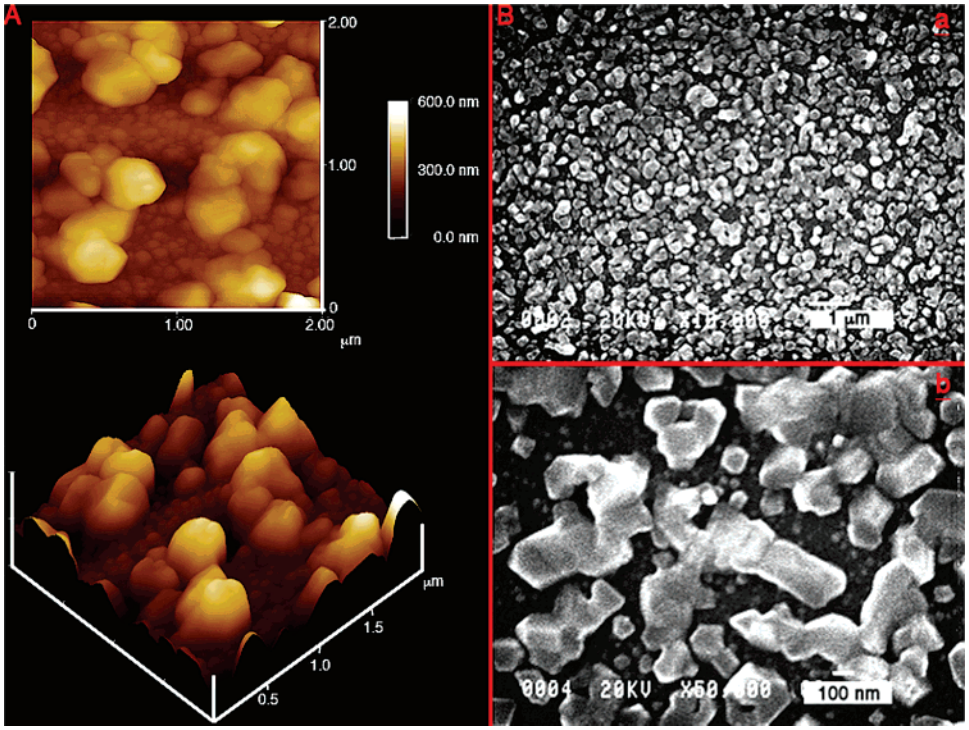

Figure 9. (A) AFM and (B) SEM at (a) ×10 000 and (b) ×50 000 magnification of maghemite made from reoxidation of Fe particles through Scheme 1, pathway c.

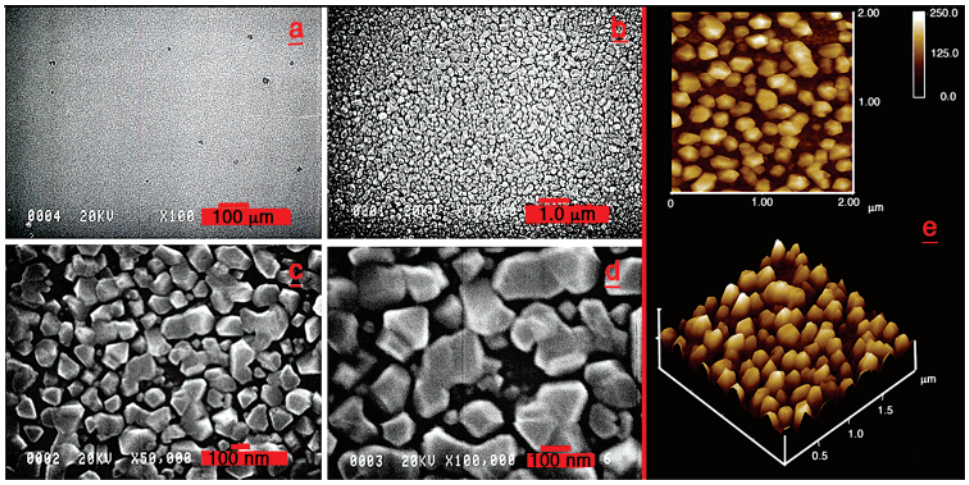

Figure 10. SEM at magnifications of (a) ×100, (b) ×10 000, (c) ×50 000, (d) ×100 000, and (e) AFM of maghemite particles made from oxidation of Fe particles via Scheme 1, pathway e.

Maghemite was characterized by XRD analysis of the films (Figure 4d,e), which showed that they are crystalline with a relatively intense [311] reflection at $2\theta = 35.6°$ and a [440] reflection at $2\theta = 62.9°$ characteristic of γ-Fe_2O_3. The XRD of the films made from Scheme 1, pathway e shows a higher degree of crystallinity (Figure 4e) as evidenced by the more intense and better resolved diffraction that also allows observation of the [511] reflection at $2\theta = 57.3°$.

Imaging of the films by SEM shows that they are characterized by an array of well-formed particles distributed on the surface. The maghemite generated in Scheme 1, pathway c, directly from the reduced Fe^{3+} oxide/hydroxide gel, has relatively irregular particles that nonetheless show evidence of facets at the edges indicative of crystalline composition, although they are probably not single crystals (Figure 9). AFM imaging of the surface morphology also reflects the faceted edges and measures an average grain diameter of 575 nm. A qualitative assessment of the SEM (Figure 9B) shows some small particles of ~100 nm; however, most are considerably larger and appear to range from about 300 to 500 nm.

Consistent with the XRD, the maghemite produced from oxidation of the Fe particles generated from hematite reduction (Scheme 1, pathway e) shows a similar morphology in the SEM (Figure 10a−d) but with better formed and more regular crystallites that appear to be of a much narrower particle size distribution. Moreover, the SEM shows them

(26) Itoh, H.; Sugimoto, T. *J. Colloid Interface Sci.* **2003**, *265*, 283.
(27) Frankamp, B. L.; Boal, A. K.; Tuominen, M. T.; Rotello, V. M. *J. Am. Chem. Soc.* **2005**, *127*, 9731.
(28) Sharma, R.; Pratima, C.; Lamba, S.; Annapoorni, S. *Pramana* **2005**, *65*, 739.

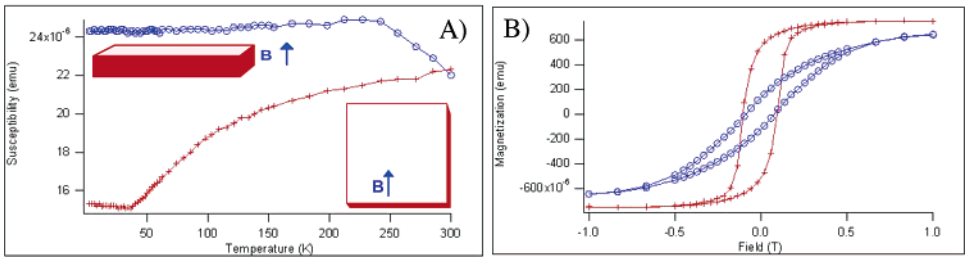

Figure 11. (A) Zero-field cooled Fe film (Scheme 1, pathway e) parallel (+) and perpendicular (○) to the magnetic field. (B) Magnetic hysteresis, recorded at 2 K, of Fe (Scheme 1) placed parallel and perpendicular to the magnetic field.

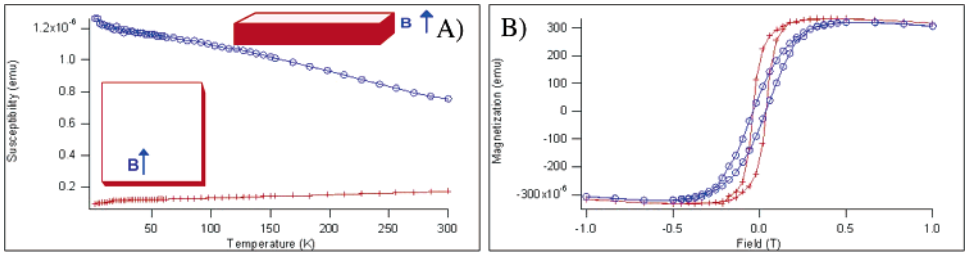

Figure 12. (A) Zero-field cooled γ-Fe_2O_3 thin film parallel (+) and perpendicular (○) to the magnetic field. (B) Magnetic hysteresis, recorded at 2 K, of γ-Fe_2O_3 placed parallel and perpendicular to the magnetic field.

to be more tightly packed with at least a qualitative semblance of order. The AFM shows closely arrayed crystallites with well-defined faces (Figure 10e). The crystallites are smaller than those generated through Scheme 1, pathway c with the particle sizes appearing to range from around 100 to 200 nm with some particles around 400 nm. The mean grain size determined from AFM grain size analysis is 271 nm.

Magnetic Properties. The Fe films made from the reduction of hematite (Scheme 1, pathway d) and the maghemite made from these Fe films (Scheme 1, pathway e) appear to exhibit the best microstructure in terms of the apparent crystallinity of the particles and the uniformity of their dispersal on the surface. These particles, however, are too large to be superparamagnetic, and no evidence of that behavior is observed. At the limit of a thin film, there is potentially a direction of long-range magnetic order in-plane and little or no ordering out-of-plane. As a result of this, the Fe samples (Figure 11) give a susceptibility typical of bulk iron in the in-plane direction, while in the out-of-plane direction, the susceptibility shows little dependence on temperature. No crystallographic orientation of the particles is expected to be present in these samples, and none is indicated by the data. In the hysteresis plots, a similar coercivity is observed in both directions with a magnitude of 0.1 and 0.09 T. The main difference lies in the magnetization direction, where the in-plane direction is the direction of easy magnetization as compared to the out-of-plane film direction. The difference in the slopes implies a more ordered magnetization in the in-plane direction. Similar effects are observed in maghemite (Figure 12), although the effect is less significant.

Conclusion

The central conclusions of this study are that high-quality thin films can be made from a new epoxide-catalyzed sol−gel approach used to making Fe^{3+} oxide/hydroxide gels. Calcination of the resulting Fe^{3+} oxide/hydroxide gel films under either inert or oxidative conditions appears to produce only hematite. As such, this differs from some of the other sol−gel gel techniques where different oxide phases can formed directly through either the choice of gelation agent or the specific processing conditions.[16] The oxide phase that does form is comparable morphologically to those formed with organic gelation agents and, in particular, is quite similar to the hematite formed from Fe^{3+} oxide/hydroxide gels containing polyvinylpyrrolidone.[12] Once formed, however, these films can be thermally processed to produce magnetic phases. Under reductive conditions, the Fe^{3+} gel films and the hematite films both leave a more-or-less continuous distribution of submicrometer Fe particles on the surface. These discrete Fe particles, if reoxidized slowly at very low O_2 concentrations, yield films composed of very well-formed maghemite crystallites, the best of which are obtained from metallic iron generated from reduction of hematite. Given the broad array of the metal ions that can be gelled using this approach, this may suggest a general route to producing metallic and oxidic thin films of a series of metals.

Acknowledgment. Funding was provided by the Air Force Office of Scientific Research through MURI 1606U8. C.-D.P. was supported by a grant from MARTECH.

CM0617079